# Effect of Multiwalled Carbon Nanotubes on the Properties of Poly(methyl methacrylate) in PMMA/CNT Nanocomposites

*Sandeep Nath Tripathi*,[1] *Sauraj Singh*,[1] *Rajender Singh Malik*,[1,2] *Veena Choudhary**[1]

**Summary:** In the present paper poly(methyl methacrylate) (PMMA)/multiwall carbon nanotubes (MWCNT) nanocomposites were prepared by bulk polymerization of MMA in presence of varying amounts of MWCNT and 2-hydroxyethyl methacrylate (HEMA) modified MWCNT (HCNT) using azobisisobutyronitrile (AIBN) as an initiator. The nanocomposites were characterized for their structural, thermal, electrical and morphological behaviour using Fourier transform infrared spectroscopy (FTIR), Raman spectroscopy, dynamic mechanical analysis (DMA), thermogravimetric analysis (TGA), differential scanning calorimetry (DSC) and scanning electron microscopy (SEM). The presence of nanofiller inhibits the formation of head to head linkages as all the nanocomposite samples show two step degradation whereas PMMA prepared under similar condition showed three step degradation. The glass transition temperature ($T_g$) of PMMA increased after incorporation of MWCNTs. The obtained nanocomposites show an increasing trend in the molecular weight with increase in the wt % of MWCNT whereas it decreases with the increasing initiator concentration. It was observed that the electrical conductivity is the function of molecular weight of the polymer as well as the content of MWCNT in the nanocomposites. The electrical conductivity of PMMA/HCNT composites was slightly lower as compared to PMMA/MWCNT whereas an increasing trend in the storage modulus of PMMA/HCNT nanocomposites was observed.

**Keywords:** electrical conductivity; multiwall carbon nanotubes; nanocomposite; 2-hydroxyethyl methacrylate; poly(methyl methacrylate)

## Introduction

Over the last two decades, carbon nanotubes have attracted much attention due to its outstanding physical, structural, mechanical and electrical properties as well as an extremely high aspect ratio with low density.[1–3] Recently researchers have focused on utilizing these extraordinary characteristics in polymeric composites, electronic devices, hydrogen storage and field emission display.[4,5]

Polymer nanocomposites are a new class of composite materials prepared by the incorporation of nanofillers such as nanoclay and carbon based fillers such as carbon nanofibre,[6] CNTs,[7] graphene[8] etc. Many of the outstanding properties of CNTs can be exploited by incorporating them into some polymer matrix in which the CNTs are used as nanofillers. Nanotubes have received interest as noble material because the incorporation of CNTs leads to a large enhancement in the electrical, thermal and mechanical properties as a result of interaction between polymer and nanotubes. In order to exploit these properties, CNTs are

[1] Centre for Polymer Science and Engineering, Indian Institute of Technology Delhi, New Delhi-110016, India
Fax: +91-11-26591421;
E-mail: veenach@hotmail.com; veenac@polymers.iitd.ernet.in
[2] Department of Chemistry, Deenbandhu Chhotu Ram University of Science and Technology Murthal, Sonepat-131039, India

 

dispersed in polymer matrix using various methods such as solution blending, melt blending[9,10] and in situ polymerization.[11,12] The composites exhibited superior thermal stability, electrical conductivity, improved stiffness and strength even at very low concentration of CNTs. In spite of this, CNTs usually exist in aggregated form in the matrix which is considered as an obstacle for many applications. To overcome this problem attempts have been made to disperse CNTs uniformly not only in the polymer matrix but also in aqueous as well as organic media by the surface modification of CNTs via covalent or non-covalent methods.[13]

The easiest way to functionalize CNT is to attach chemical groups (e.g. –COOH, -OH etc) by oxidation using nitric acid ($HNO_3$)[14] and sulphuric acid ($H_2SO_4$)[15] or oxidation reactions in air.[16] The oxidation resulted in the defects in the wall structure to introduce carboxyl, hydroxyl, carbonyl groups etc. which can be used for further functionalization by other molecules. Gogotsi et al[17] have reported the oxidation of MWCNT in air and acids by varying the time and temperature. The structural changes that occur during oxidation of MWCNTs were monitored using Raman spectroscopy. The intensity ratios of D and G bands were used to estimate the concentration of defects. Aviles et al[18] have used mild acid treatment method to oxidize MWCNTs where they used $H_2SO_4$, $HNO_3$ and $H_2O_2$ at varying concentration. A number of thermoplastics have been used for the incorporation of CNTs to prepare polymer/CNT nanocomposites to improve the electrical and mechanical properties e.g. PMMA,[9,19] polystyrene,[20,21], polycarbonate[22] and others.[23,24] A limited number of research papers are available in which functionalized CNTs have been used as filler. Yuen et al [25] reported the preparation of MWCNT/PMMA nanocomposites using *in situ* and *ex situ* methods. SEM micrographs reveal that the MWCNT/PMMA composites prepared using *in situ* adheres better than those prepared using *ex situ*. *In -situ* polymerization methods used for the preparation of MWCNT/PMMA composites exhibit a lower electrical resistivity and a lower percolation threshold than those prepared in *ex situ* system. Krishnamoorti et al[26] have prepared PMMA/SWCNT nanocomposites by in situ polymerization where they found that the addition of less than 0.1 wt % SWNT to PMMA led to an increase in the low-temperature elastic modulus of approximately 10% beyond that of pure PMMA whereas $T_g$ and storage modulus remains unchanged. Kumar et al[27] have reported a method for the functionalization of multi-walled carbon nanotubes (MWCNTs) with a biomedically important polymer, poly(2-hydroxyethyl methacrylate) poly (HEMA), by chemical grafting of HEMA monomer followed by free radical polymerization.

In this paper we report the preparation and characterization of PMMA nanocomposites based on MWCNT and HCNT (HEMA modified MWCNT) using azobisisobutyronitrile (AIBN) as an initiator. In order to investigate the effect of molecular weight on electrical properties of PMMA/MWCNT nanocomposites were prepared by taking varying amounts of AIBN and fixed concentration of MWCNTs. To see the effect of functionalization of carbon nanotubes and its content, nanocomposites were prepared using varying amounts of MWCNT and HCNTs and characterized for their thermal stability, electrical conductivity, morphology and thermomechcanical property. Functionalization had significant effect on the electrical conductivity which was slightly lower in case of PMMA/HCNT nanocomposite as compared to PMMA/MWCNTs whereas the storage modulus and glass transition increased significantly.

## Experimental Part

### Materials

Methyl methacrylate [MMA, ~99% purity, CDH] was purified by washing with aqueous solution of NaOH (5% w/v) to remove the inhibitor followed by washing with

 

distilled water until neutral pH and then dried over anhydrous $Na_2SO_4$. Finally it was distilled under vacuum to get pure MMA. The free radical initiator AIBN with purity >97% (Spectrochem) was used after recrystallization. All other chemicals of reagent grade were used as received.

MWCNTs (Nanocyl NC7000) was purchased from Nanocyl S.A., Belgium manufactured via a chemical vapor deposition (CVD) process, with carbon purity of ~90%, average diameter ~9.5 nm, and average length ~1.5 μm.

### Preparation and Characterization of Functionalized MWCNTs

Modified MWCNT were prepared according to the reaction scheme (Scheme 1). The procedure used was as follows:

i. For oxidative treatment, MWCNTs (0.5 g) dispersed in 80 ml acid solution ($HNO_3 + H_2SO_4$ 8M) was placed in 100 ml round bottom flask fitted with a reflux condenser. The mixture was stirred using magnetic stirrer and heated in an oil bath at 60 °C for 15 min. The mixture was then subjected to ultra sonication (100 W) for 2 h. The slurry was filtered and thoroughly washed with distilled water till neutral pH and then dried in vacuum oven at 100 °C for ~8 h.[18]

ii. 500 mg of oxidized MWCNTs were stirred at reflux temperature with an excess amount (25 mL) of thionyl chloride under nitrogen atmosphere for 24 h. Excess thionyl chloride was removed by distillation, subsequently dried under vacuum to give the acid chloride-functionalized MWCNTs (MWCNT-COCl).

iii. Then 2 mL of HEMA and 1 mL of triethyl amine were mixed with the acid chloride functionalized MWCNTs (prepared in step 2) dispersed in 10 mL of anhydrous THF. Triethyl amine was used as acid scavenger. This mixture was stirred for 6 h at ambient temperature under nitrogen atmosphere. The resultant solid was filtered and washed with acetone and dried in the vacuum oven at 40 °C overnight to get HEMA modified MWCNT (designated as HCNTs).[27]

Structural and morphological characterization of MWCNTs and HCNTs was done using FTIR, Raman, SEM and TEM

### Preparation of PMMA Nanocomposites Using MWCNT/HCNT as Filler

#### *Preparation of PMMA/MWCNT Nanocomposites*

To see the effect of molecular weight, PMMA nanocomposites were prepared by in situ bulk polymerization of MMA using varying amounts of AIBN as initiator and a fixed concentration of MWCNTs (1 wt %). In the second set of experiments, we prepared PMMA/MWCNT nanocomposites by similar procedure using fixed concentration of AIBN (2 wt %) and varied the MWCNTs content.

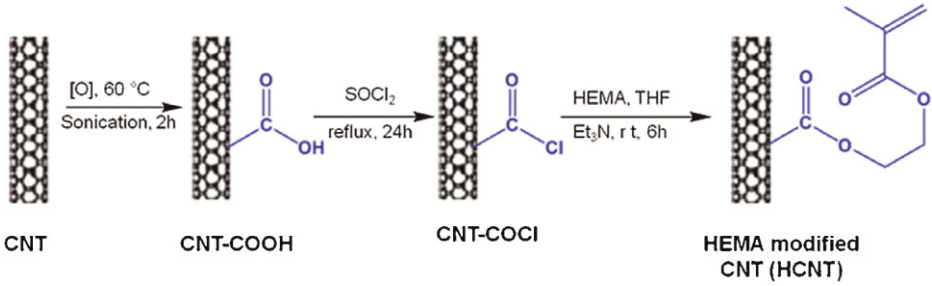


***Scheme 1.***
Schematic of functionalization of MWCNT.

 

i. Effect of Initiator Concentration (MWCNT 1 wt %)
In the first set of experiments, PMMA/MWCNT nanocomposites were prepared by taking 10g of MMA monomer and 0.1g of MWCNTs in the test tube. It was sonicated for 1 h to get a homogeneous dispersion followed by using varying amounts of AIBN i.e. [0.1, 0.5, 1.0, 1.5 and 2.0 wt%]. The reaction mixture was purged with nitrogen to remove the dissolved oxygen and the polymerization was carried out at 70 °C in an oil bath for 4h followed by heating in a hot air oven at 100 °C for 6 h. The samples prepared using 0.1, 0.5, 1.0, 1.5 and 2.0 wt %] AIBN were designated as PCNTA-1, PCNTA-5, PCNTA-10, PCNTA-15 and PCNTA-20 respectively. The numerical suffix represents the percent concentration of AIBN multiplied by 10.

ii. Effect of MWCNT (AIBN 2 wt%)
In the second set of experiments, we kept the concentration of AIBN fixed as 2 wt% and several PMMA/MWCNT nanocomposite samples were prepared by taking varying amounts of MWCNT [i.e. 0.1, 0.5, 1.0, 1.5 and 2.0 wt%] in the initial feed. Similar procedure was used to prepare samples having varying amounts of MWCNTs. The samples prepared using 0.1, 0.5, 1.0, 1.5 and 2.0 wt% MWCNTs were designated as PCNT-1, PCNT-5, PCNT-10, PCNT-15 and PCNT-20 respectively. In these sample designation the numerical suffix represent the percent concentration of MWCNTs multiplied by 10.

*Preparation of PMMA/HCNT Nanocomposites*

PMMA/HCNT nanocomposites were prepared by using the same procedure as above to get the covalently functionalized nanocomposites, i.e. at fixed concentration of AIBN (2 wt%) and varying amounts of HCNTs (i.e. 0 to 2.0 wt %). First a given amount of HCNT was dispersed in MMA and sonicated for 1 h at room temp followed by the addition of AIBN as an initiator (2 wt %). The reaction mixture was heated in an oil bath at 70 °C for 4 h followed by heating for 6h in an air oven at 100 °C for complete polymerization. The nanocomposites were crushed and then sheets were compression molded for analysis. The samples prepared using 0.1, 0.5, 1.0, 1.5 and 2.0 wt% HCNTs were designated as PHCNT-1, PHCNT-5, PHCNT-10, PHCNT-15 and PHCNT-20 respectively.

## Characterization Techniques

Infrared spectra (FTIR) were recorded on a *Perkin Elmer* FTIR spectrometer using KBr as a background.

*Renishaw InVia* Raman microscope was used for recording Raman spectrum of samples. These spectra were recorded using diode laser at 514 nm excitation with Raman shift between 100 $cm^{-1}$ - 3000 $cm^{-1}$.

Waters gel permeation chromatograph (GPC) was used for the molecular characterization using THF as solvent and polystyrene samples of known molecular weight as standards. The nanocomposite samples were dissolved in THF followed by centrifugation at 12000 rpm and then filtered using 0.45 μm PTFE syringe filter before injection.

Thermal stability of PMMA in presence of varying amounts of MWCNTs was evaluated by recording thermogravimetric (TG) traces in nitrogen atmosphere. *Perkin Elmer Pyris 6 TGA* was used for recording TG traces. A heating rate of 20 °C/min and a sample size of $5 \pm 1$ mg were used in each experiment.

TA instruments *Q-200* differential scanning calorimeter (DSC) was used for recording DSC scans (heating and cooling) under $N_2$ atmosphere. About 5-6 mg of samples was first heated from room temperature to 170 °C at a heating rate of 10 °C /min. followed by quench cooling and then recording second heating scans at a heating rate of 10 °C /min.

 

TA instruments *Q-800* dynamic mechanical analyzer equipped with single cantilever in bending mode was used for recording DMA curves in the temperature range of 30 °C to 150 °C. A heating rate of 5°C/min and frequency 1 Hz were used for recording DMA curves. Rectangular specimens having dimensions of 40 mm length, 13 mm width and 2.5 mm in thickness were used.

For morphological characterization, SEM images were taken using *EVO-50* scanning electron microscope. Manually fractured compression molded samples were used for this purpose. The samples were coated first with silver and then by gold with sputtering device before observation.

The DC electrical conductivity of nanocomposite samples (rectangular strips of dimensions $13 \times 7 \times 1.5$ mm$^3$) at ambient temperature was measured using four probe method. The experiment was performed using *Keithley 4200* semiconducting characterization system.

## Results and Discussion

### Characterization of MWCNT/HCNT

#### *Dispersion Test*

The functionalization of MWCNT with carboxyl and other oxygen functionalities was characterized by its dispersion test, where acid treated MWCNTs and as received MWCNTs (15 mg) were dispersed in 10 mL of ethanol followed by ultrasonication for 1h and the solution was kept at room temperature. After 24h it was observed that the as-received MWCNTs settle down whereas the acid-treated MWCNTs remains dispersed (in fact no settling was observed even after 1 month). This may be due to the hydrogen bonding between oxygen functionalities present in the acid treated MWCNTs and solvent molecule whereas there is no interaction between as received MWCNTs and solvent molecule (Figure 1).

#### *Energy Dispersive X-Ray Spectroscopy*

The elemental analysis was carried out using *EVO 50 electron microscope* enabled with energy dispersive X-ray (EDX) spectroscopy. The EDX analysis showed that after acid treatment, % oxygen increased from 3.9 (as received) to 8.55% [MWCNT-COOH] which strongly supported the presence of oxygen functionalities on to the surface of MWCNTs. The results are summarized in Table 1.

Acid treated MWCNTs was further modified using 2-hydroxyethyl methacrylate

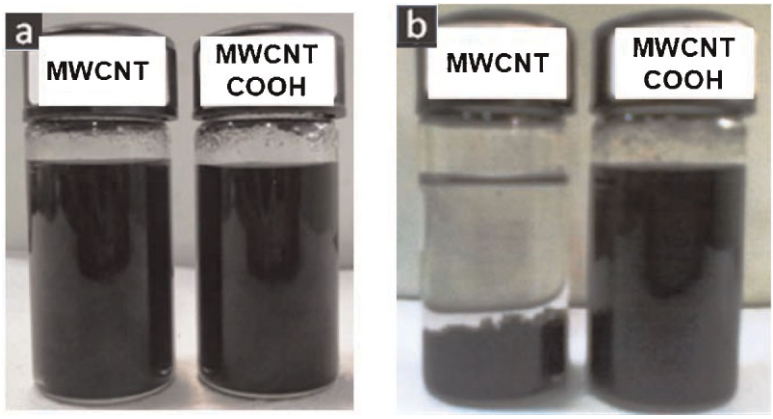


***Figure 1.***
Dispersion of MWCNT and acid treated MWCNT after 1h sonication at room temperature (a) after sonication (b) after 24h.

 

***Table 1.***
Results of EDX analysis of MWCNTs before and after acid treatment.

| Sample designation | C (atomic %) | O (atomic %) | Fe (atomic %) | Others (atomic %) |
|---|---|---|---|---|
| MWCNT | 95.50 | 3.90 | 0.09 | 1.41 |
| MWCNT-COOH | 89.00 | 8.55 | 0.07 | 2.38 |

***Table 2.***
Results of TG analysis for MWCNT and HCNT in N2 atmosphere.

| Temperature range (°C) | Mass loss (%) | |
|---|---|---|
| | MWCNT | HCNT |
| 100–500 | 4.0 | 8.0 |
| 500–800 | 1.5 | 2.0 |

(HEMA) to get vinyl terminated MWCNTs i.e. HEMA modified MWCNTs (HCNT) which was characterized using FTIR, Raman spectroscopy and TGA analysis. .

*FT-IR Analysis*

FT-IR spectra of MWCNT and HCNT are shown in Figure 2. FT-IR spectrum of raw MWCNTs shows characteristic peaks of O-H and C=C stretching at 3420 and 1630 $cm^{-1}$ respectively, due to the presence of small amount of oxygen containing functional groups. FT-IR spectra of HCNT show the characteristic absorption at 1727 $cm^{-1}$and 1625 $cm^{-1}$ due to (C = O, C=C stretching) and also band at 1385 $cm^{-1}$ corresponding to the bending vibrations of C–H bonds in $–CH_3$ groups, confirming the presence of methacrylic groups in HCNTs. Narrow band of an intermediate intensity observed at 1465 $cm^{-1}$ is attributed to O–C = O groups. Availability of C–O–C bonds and –OH groups attached to benzene rings is confirmed by the bands at 1095 and 1022 $cm^{-1}$. The absorption band with maximum at 1369 $cm^{-1}$ is attributed to vibrations of C–H bonds in $–CH_2–OH$ groups and bands at 1570 and 1480 $cm^{-1}$ corresponding to C–H vibrations in substituted benzene ring were also observed. These structural changes observed confirms the formation of functionalized MWCNTs which was also supported by Raman spectroscopy.

*Raman Spectroscopy*

Raman spectra of MWCNTs and HCNTs are shown in Figure 3. In the Raman spectra,

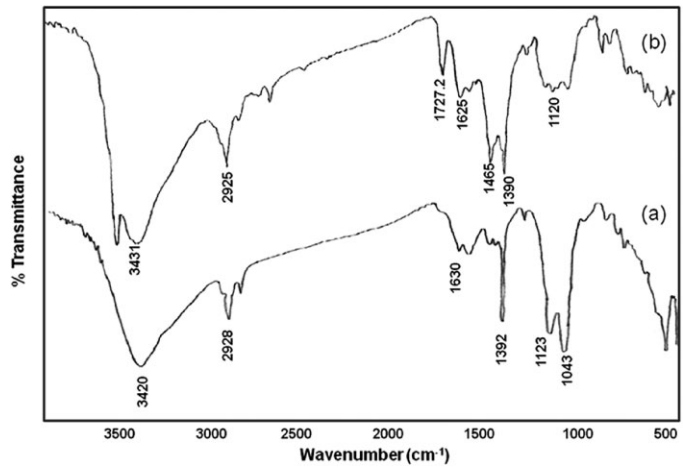


***Figure 2.***
FTIR spectra of (a) MWCNT and (b) HCNT.

 

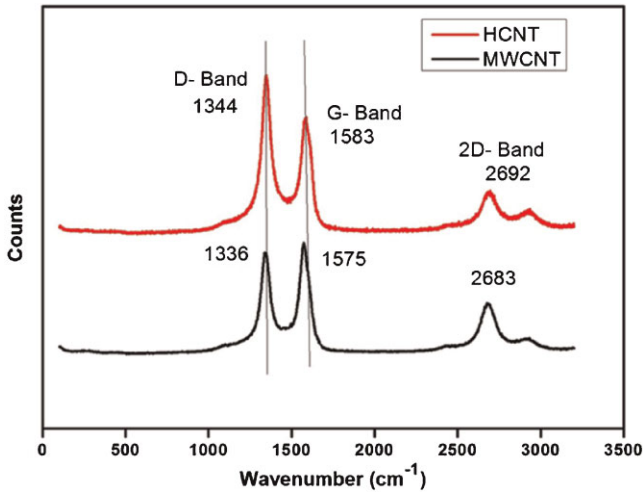


***Figure 3.***
Raman spectra of MWCNT and HCNT.

peaks at 1336 $cm^{-1}$ (D band and corresponds to disordered graphitic structure $sp^3$ hybridized state of carbon) and 1575 $cm^{-1}$ (G band which correspond to the graphitic structure of carbon nanotubes i.e. $sp^2$ state) were observed. When the nanotubes were functionalized some of the benzene ring opens up which created distortion in the graphitic structure and thus increasing the intensity of D band. This causes shift in the position as well as intensity of D and G bands. The intensity ratio i.e. $I_D/I_G$ in case of MWCNT was found to be 0.95 whereas for HCNT it was 1.33. This observation confirms the functionalization of MWCNT and is also supported by dispersion test.

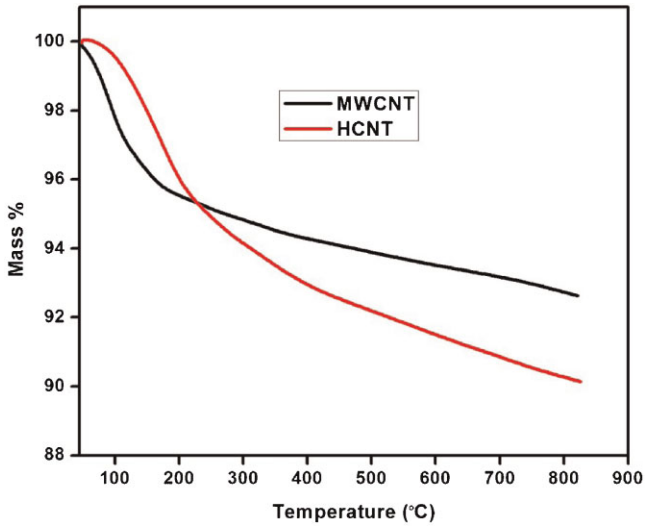


***Figure 4.***
TG traces of MWCNTs and HCNTs.

 

*Thermogravimetric Analysis*

Figure 4 shows the TG traces of MWCNT and HCNT. Thermogravimetric analysis also reflected the successful functionalization of MWCNTs. The thermal stability of MWCNT and HCNT was compared by comparing the % mass loss in the temperature range 100-500 and 500-800 °C. The maximum mass loss was 4% for MWCNT and 8% in case of HCNT in the temperature range of 100-500 °C which may be due to the oxygen functionalities or due to the presence of aliphatic group thus confirming the presence of organic functionalities on the surface of MWCNTs.

## Characterization of PMMA/MWCNT and PMMA/HCNT Nanocomposites

*Molecular Characterization*

i. Effect of AIBN Concentration
To investigate the effect of AIBN concentration on the characteristic of PMMA/MWCNT (1 wt %) nanocomposites, several samples were prepared by taking 0.1, 0.5, 1.0, 1.5 and 2.0 wt% AIBN as an intiator. The results of number average/weight average molecular weight as determined by GPC are summarized in Table 3.
As expected, molecular weight decreased with increasing concentration of AIBN. On the other hand polydispersity index increased. Nanocomposites prepared using 2 wt % AIBN showed much higher molecular weight as compared to PMMA prepared under similar conditions. From these results it can be concluded that the presence of nanotubes inhibits the termination reaction. This could be due to the increased viscosity of the system in presence of nanotubes as compared to neat PMMA. It has been reported by Wang and Choi's group that during in situ polymerization, the radicals of AIBN not only initiate the polymerization of monomers but also opens up the pi-bonds of CNT, which results in the grafting of polymer chains on the surface of CNTs caused by either attachment of oligomeric PMMA chains or by direct polymerization of MMA at the opened pi-bond,[28,29] which may leads to the increase in the molecular weight of the polymer in the PMMA/MWCNT nanocomposites.

ii. Effect of MWCNTs
In order to investigate the effect of MWCNTs content on the properties of PMMA, we kept the concentration of AIBN constant as 2 wt % and MWCNT content was varied as 0.1, 0.5, 1.0, 1.5, 2.0 wt %. The results of GPC are given in Table 4.

The molecular weight as well as polydispersity index of PMMA increased with increasing MWCNT content in the nanocomposites. It could be due to the increased viscosity of the system in presence of nanotubes which in turn inhibits the termination reaction.

The results of molecular weight and molecular weight distribution for samples prepared using varying amounts of HCNTs at fixed AIBN concentration (2 wt%) are

***Table 3.***
Effect of AIBN concentration on the molecular weight of PMMA in PMMA/MWCNT nanocomposites (MWCNT content 1 wt %).

| Sample designation | AIBN (wt %) | $M_n$ (g/mol) | $M_w$ (g/mol) | Mw/Mn | Conductivity (σ) S/cm |
|---|---|---|---|---|---|
| PMMA | 2.0 | $3.9 \times 10^4$ | $7.5 \times 10^4$ | 1.9 | $1.02 \times 10^{-9}$ |
| PCNTA-1 | 0.1 | $5.9 \times 10^5$ | $1.1 \times 10^6$ | 1.9 | – |
| PCNTA-5 | 0.5 | $2.5 \times 10^5$ | $4.9 \times 10^5$ | 1.9 | $1.05 \times 10^{-5}$ |
| PCNTA-10 | 1.0 | $1.7 \times 10^5$ | $4.8 \times 10^5$ | 2.7 | $5.77 \times 10^{-5}$ |
| PCNTA-15 | 1.5 | $7.7 \times 10^4$ | $3.0 \times 10^5$ | 3.8 | $7.94 \times 10^{-5}$ |
| PCNTA-20 | 2.0 | $7.4 \times 10^4$ | $2.9 \times 10^5$ | 3.9 | $1.08 \times 10^{-4}$ |

 

*Table 4.*
GPC results of PMMA/MWCNTs nanocomposites (at 2 wt % AIBN).

| Sample designation | MWCNT (wt %) | $M_n$ (g/mol) | $M_w$ (g/mol) | $M_w/M_n$ |
|---|---|---|---|---|
| PCNT-1 | 0.1 | $6.3 \times 10^4$ | $1.95 \times 10^5$ | 3.0 |
| PCNT-5 | 0.5 | $7.0 \times 10^4$ | $2.42 \times 10^5$ | 3.5 |
| PCNT-10 | 1.0 | $7.4 \times 10^4$ | $3.28 \times 10^5$ | 4.4 |
| PCNT-15 | 1.5 | $7.8 \times 10^4$ | $3.08 \times 10^5$ | 3.9 |
| PCNT-20 | 2.0 | $8.0 \times 10^4$ | $3.34 \times 10^5$ | 4.4 |

summarized in Table 5. At any given concentration of CNTs, PMMA/HCNT composite samples had higher $M_n$ values and lower polydispersity index as compared to PMMA/MWCNT composites.

The molecular weight of PMMA in PMMA/HCNT nanocomposites also showed an increase with increasing concentration of HCNTs. This could be due to the presence of vinyl group on the surface of MWCNTs, polymer chains will grow directly from the surface of nanotubes and also the presence of nanotubes will increase the viscosity of the system which may be responsible for higher molecular weight and narrow polydispersity index.

### *Electrical Conductivity*

The above nanocomposites have been tested for their electrical conductivity to see the effect of molecular weight, MWCNT and HCNT content on the conductivity. The results of electrical conductivity of PMMA/MWCNT (1 wt %) as a function of molecular weight are given in Table 3. A significant increase in conductivity from $10^{-9}$ to $10^{-4}$ S/cm was observed. It increased with decrease in molecular weight and it was maximum when nanocomposite was prepared using 2 wt % AIBN as initiator. The increase in conductivity with decrease in molecular weight could be due to the better dispersion of CNTs in the PMMA matrix. Therefore all other studies were carried out using 2 wt % AIBN concentration. Figure 5 shows the DC electrical conductivity ($\sigma$) for PMMA/MWCNT nanocomposites with/without modified MWCNTs at room temperature. The results show that the electrical conductivity of PMMA was found to increase on incorporation of MWCNT/HCNT and a sharp increase in the conductivity was observed between 0 to 0.5 wt percent of CNT loading which can be attributed to the formation of conducting percolation network throughout the matrix. At any given concentration the value of "$\sigma$" for PMMA/HCNTs nanocomposites was slightly lower as compared to PMMA/MWCNTs nanocomposites. One would have expected higher conductivity using modified MWCNTs as this can led to better dispersion and better interaction between filler and matrix, however the lower values observed could be due to the decrease in aspect ratio /or increase in defect structures of HCNTs. The electrical conductivity for PMMA/MWCNTs having 0.5 wt % of MWCNT [PCNT-5] ($1.48 \times 10^{-4}$ (S/cm) was much higher as compared to neat

*Table 5.*
GPC results of PMMA/HCNTs nanocomposites.

| Sample designation | HCNT (wt %) | $M_n$ (g/mol) | $M_w$ (g/mol) | Mw/Mn |
|---|---|---|---|---|
| PHCNT-1 | 0.1 | $7.4 \times 10^4$ | $1.25 \times 10^5$ | 1.7 |
| PHCNT-5 | 0.5 | $7.6 \times 10^4$ | $1.44 \times 10^5$ | 1.9 |
| PHCNT-10 | 1.0 | $7.9 \times 10^4$ | $1.5 \times 10^5$ | 1.9 |
| PHCNT-15 | 1.5 | $8.4 \times 10^4$ | $1.0 \times 10^5$ | 1.3 |
| PHCNT-20 | 2.0 | $8.8 \times 10^4$ | $1.6 \times 10^5$ | 1.8 |

 

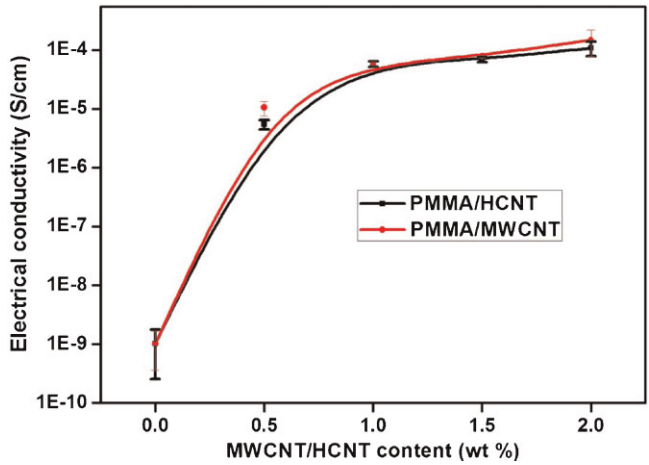


***Figure 5.***
Electrical conductivity for PMMA/MWCNT and PMMA/HCNT nanocomposites.

PMMA $1.02 \times 10^{-9}$ (S/cm). Overall the conductivity of nanocomposites satisfies the antistatic criteria and can be used for electrostatic dissipation.

### Thermal Characterization

i. Differential Scanning Calorimetry
Figure 6 and Figure 7 show the DSC traces for PMMA/MWCNTs and PMMA/HCNTs nanocomposites respectively. $T_g$ was measured as the mid-point inflection. A significant increase in $T_g$ was observed at a loading of 2 wt % MWCNT [sample PCNT-20]. An increase in $T_g$ at higher loadings of MWCNT could be due to some interactions of MWCNT with the polymer matrix which in turn restricts the mobility of polymer chains [Figure 6]. At any given concentration, the glass transition temperature of PMMA/HCNTs nanocomposites was higher than that of PMMA/MWCNT nanocomposites. The overall increase in $T_g$ was 15 °C and 22 °C for 2 wt % MWCNT [sample PCNT 20] and HCNT

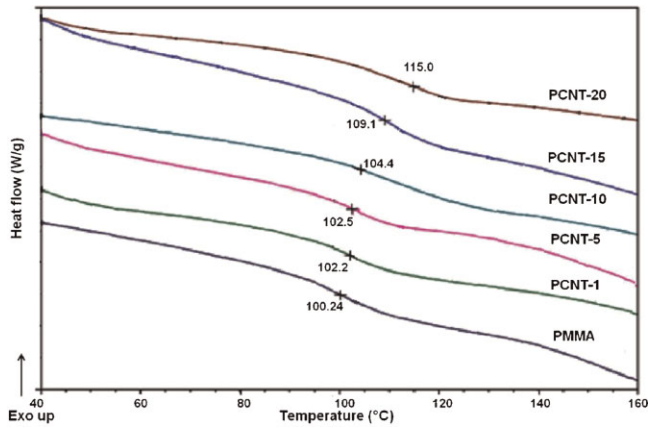


***Figure 6.***
DSC scans of PMMA/MWCNT nanocomposites.

 

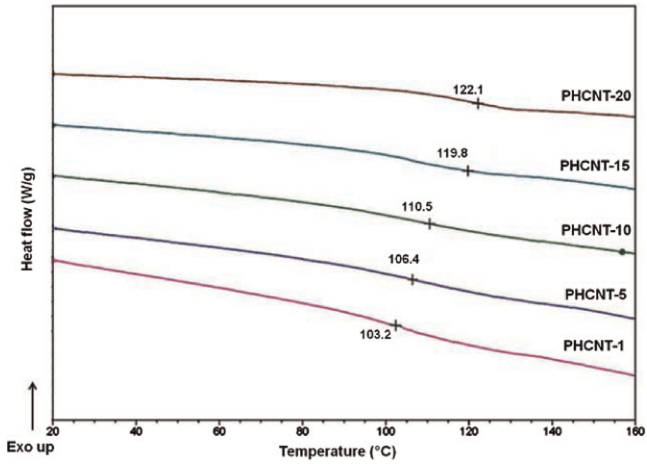


***Figure 7.***
DSC scans of PMMA/HCNT nanocomposites.

(PHCNT 20) respectively. Higher $T_g$ observed in case of PMMA/HCNT composites could be due to the covalent bonding which might have better reinforcing effect [Figure 7].

ii. Thermogravimetric Analysis
The results of TG/DTG traces for PMMA/MWCNTs and PMMA/HCNTs nanocomposites having varying amounts of MWCNTs recorded at a heating rate of 20 °C/min in nitrogen atmosphere are shown in Table 6 and Table 7. All the nanocomposite samples show two step degradation whereas three step degradation was observed in case of PMMA (Figure 8). The relative thermal stability was compared by comparing the initial degradation temperature [$T_{onset}$], temperature of maximum rate of mass loss [$T_{max}$] and final degradation temperature [$T_{end}$]. In the final step degradation, $T_{max}$ and $T_{end}$ increased upon incorporation of MWCNTs and maximum increase was observed at a loading of 1.5 wt % [sample PCNT-15]. These results also show that in the presence of MWCNTs, formation of head to head linkages is hindered and the higher degradation temperature observed in composites could be due to enhanced viscosity of matrix or inhibition of evolution of volatile products due to the presence of MWCNTs/HCNTs.

iii. Dynamic Mechanical Analysis
The thermomechcanical properties of pure PMMA and its nanocomposites

***Table 6.***
Results of TG/DTG traces for PMMA/MWCNTs nanocomposites.

| Sample designation | 1st step degradation | | | 2nd step degradation | | | 3rd step degradation | | |
|---|---|---|---|---|---|---|---|---|---|
| | $T_{onset}$ (°C) | $T_{max}$ (°C) | $T_{end}$ (°C) | $T_{onset}$ (°C) | $T_{max}$ (°C) | $T_{end}$ (°C) | $T_{onset}$ (°C) | $T_{max}$ (°C) | $T_{end}$ (°C) |
| PMMA | 177 | 188 | 211 | 279 | 301 | 319 | 349 | 348 | 406 |
| MWCNT | 558 | 572 | 594 | – | – | – | – | – | – |
| PCNT-1 | – | – | – | 260 | 302 | 318 | 349 | 375 | 401 |
| PCNT-5 | – | – | – | 267 | 302 | 315 | 350 | 378 | 401 |
| PCNT-10 | – | – | – | 269 | 303 | 321 | 349 | 380 | 406 |
| PCNT-15 | – | – | – | 270 | 281 | 309 | 356 | 397 | 421 |
| PCNT-20 | – | – | – | 274 | 303 | 317 | 348 | 379 | 401 |

 

***Table 7.***
Results of TG/DTG traces for PMMA/HCNTs nanocomposites.

| Sample designation | 1st step degradation | | | 2nd step degradation | | | 3rd step degradation | | |
|---|---|---|---|---|---|---|---|---|---|
| | $T_{onset}$ (°C) | $T_{max}$ (°C) | $T_{end}$ (°C) | $T_{onset}$ (°C) | $T_{max}$ (°C) | $T_{end}$ (°C) | $T_{onset}$ (°C) | $T_{max}$ (°C) | $T_{end}$ (°C) |
| PMMA | 177 | 188 | 211 | 279 | 301 | 319 | 349 | 348 | 406 |
| MWCNT | 558 | 572 | 594 | – | – | – | – | – | – |
| PHCNT-1 | – | – | – | 259 | 297 | 305 | 375 | 393 | 414 |
| PHCNT-5 | – | – | – | 261 | 297 | 306 | 377 | 393 | 415 |
| PHCNT-10 | – | – | – | 267 | 299 | 315 | 360 | 396 | 415 |
| PHCNT-15 | – | – | – | 269 | 294 | 303 | 375 | 390 | 414 |
| PHCNT-20 | – | – | – | 270 | 297 | 318 | 349 | 379 | 405 |

with varying weight percent of MWCNT/HCNTs were measured as a function of temperature by dynamic mechanical analysis. The plot of storage modulus and tan δ as a function of temperature for neat PMMA and nanocomposites are shown in Figure 9. It was found that in both glassy and rubbery region the storage modulus of all the nanocomposites was higher than that of neat PMMA. The increase was much higher in case of PMMA/HCNTs composites [Figure 9(c)] as compared to PMMA/MWCNTs composites [Figure 9(a)]. This could be due to better interfacial bonding between HCNTs and polymer as compared to unmodified MWCNTs. The results of storage modulus are given in 8 and 9. This was further confirmed from the values of glass transition temperature which was higher in case of PHCNT composites as compared to PCNT composites. The peak temperature in tan δ curve was noted as

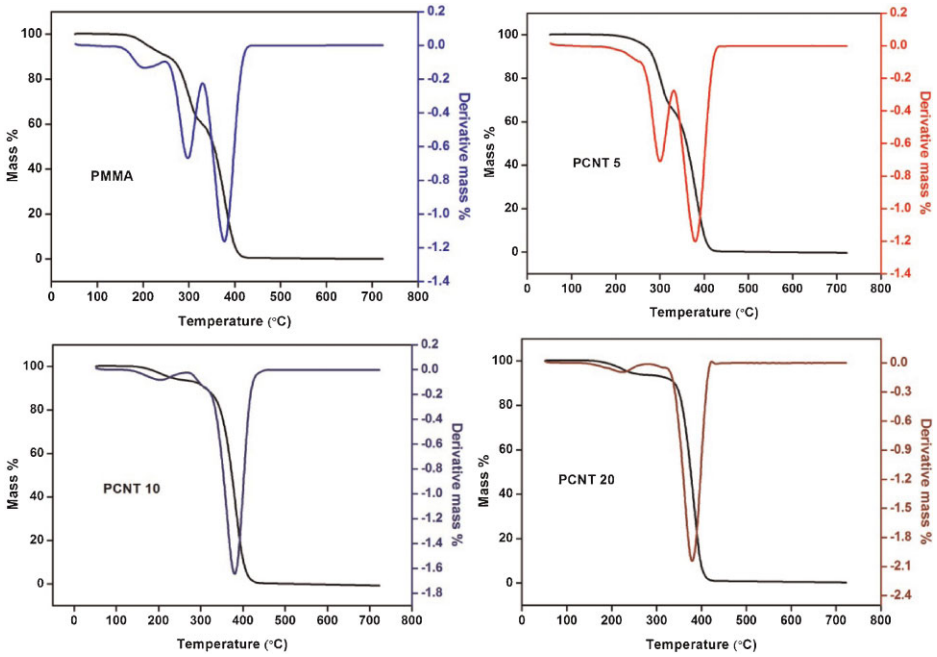


***Figure 8.***
TG/DTG traces of PMMA and PMMA/MWCNT nanocomposites.

 

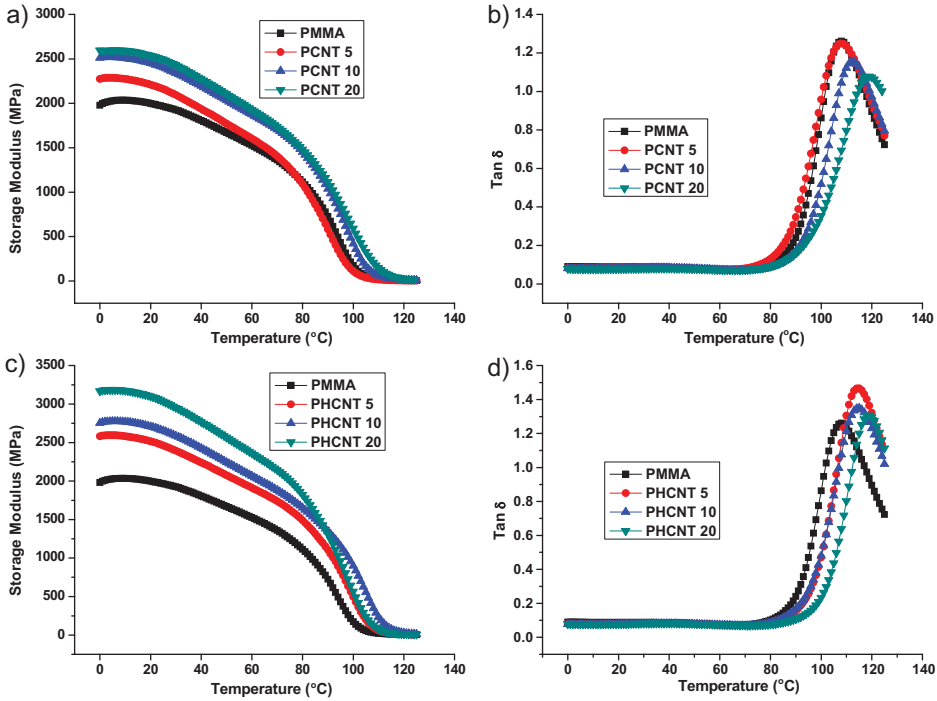


***Figure 9.***
Storage modulus and tan δ vs temperature for PMMA/MWCNT (a. b) and PMMA/HCNT (c, d) nanocomposites.

glass transition temperature and the results are given in Table 8 and 9 [Figure 9(b, d)]. As expected $T_g$ showed an increase with increasing amount of MWCNT. The tan δ peak for the PMMA/HCNT composite is shifted to a higher temperature corresponding to the large increase in $T_g$, which is further attributed to the enhanced interaction between matrix and dispersed phase in case of nanocomposite prepared using HCNT. This reinforcement efficiency has eventually been illustrated by the reinforcement effectiveness parameter (C)[30] calculated using the following equation.

$$C = \frac{\frac{Eg}{Er}composite}{\frac{Eg}{Er}matrix} \quad (1)$$

Where $E_g$ and $E_r$ are the storage modulus in the glassy and the rubbery region respectively. The higher the value of C, lower the effectiveness of the filler. The $E_g$ values were taken at 20 °C and the $E_r$ as

***Table 8.***
Results of storage modulus and Tg for PMMA/MWCNTs nanocomposites.

| Sample designation | $T_g$ (°C) | Storage modulus (MPa) at temperature (°C) | | |
|---|---|---|---|---|
| | | 20 | 80 | 100 |
| PMMA | 110 | 1998 | 1084 | 172 |
| PCNT-5 | 112 | 2210 | 1091 | 111 |
| PCNT-10 | 116 | 2452 | 1454 | 420 |
| PCNT-20 | 120 | 2537 | 1479 | 591 |

***Table 9.***
Results of storage modulus and Tg for PMMA/HCNTs nanocomposites.

| Sample designation | T g (°C) | Storage modulus (MPa) at temperature (°C) | | |
|---|---|---|---|---|
| | | 20 | 80 | 100 |
| PMMA | 110 | 1998 | 1084 | 172 |
| PHCNT-5 | 116 | 2517 | 1489 | 496 |
| PHCNT-10 | 118 | 2708 | 1654 | 899 |
| PHCNT-20 | 122 | 3101 | 1823 | 566 |

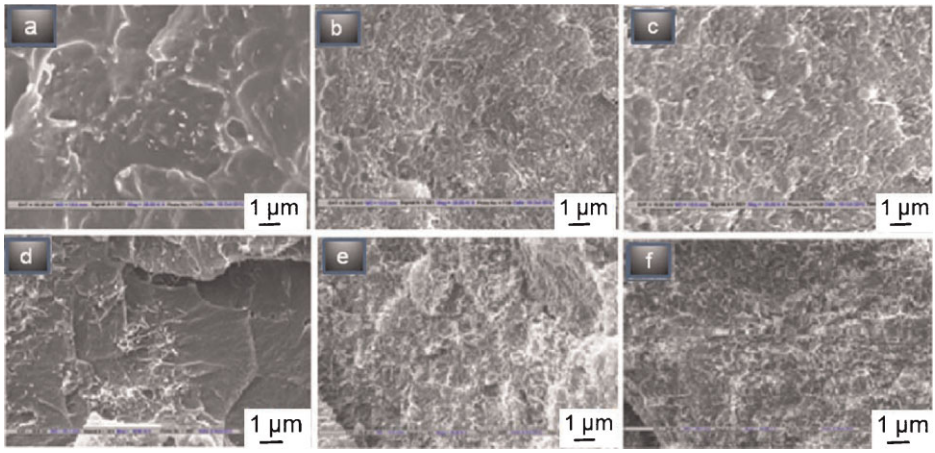


***Figure 10.***
SEM micrographs of PMMA/MWCNT (a) 0.5 wt% (b) 1 wt% (c) 2 wt% and PMMA/HCNT (d) 0.5 wt% (e) 1 wt% (f) 2 wt% nanocomposites.

the modus at 120 °C. It was found that the reinforcement effectiveness of the nanocomposites decreases as the filler loading increases e.g. at 0.5 wt% and 1.0 wt% loading the value of "C" for PMMA/MWCNT nanocomposite was 0.77 and 0.44 whereas it was 0.61 and 0.23 in case of PMMA/HCNT nanocomposite respectively. From these results one can say that HCNT shows better reinforcing effect as compared to MWCNT which is also supported by the higher glass transition temperature in case of PMMA/HCNT nanocomposites.

### *Morphological Characterization*

The morphology of the nanocomposites was investigated using EVO-50 scanning electron microscope to see the dispersion of MWCNTs and HCNTs in the PMMA matrix. Figure 10 shows SEM images for the fractured surface of PMMA/MWCNT and PMMA/HCNT nanocomposites. The SEM images clearly show the uniform dispersion of nanotubes in the PMMA matrix. Nanotubes were found highly curved and agglomerated because of the intrinsic van der Waals attractions between the individual nanotubes. Some bundles of the nanotubes were pulled out of the PMMA matrix (in PMMA/MWCNT) which may be due to the poor interaction between matrix and nanotubes and some bundles were uniformly dispersed (in PMMA/HCNT).

## Conclusion

From these results it can be concluded that the conductivity of PMMA can be enhanced by about five orders of magnitude by incorporation of very low concentration [0.5 wt %] of MWCNTs. Surface modification of MWCNTs resulted in an increase in $T_g$ and decrease in electrical conductivity. Increase in storage modulus showed that incorporation of MWCNTs act as reinforcing agent and stiffening of matrix was higher in presence of HCNTs as compared to MWCNTs which is also supported by the higher glass transition temperature in presence of HCNTs.

*Acknowledgement:* University grant commission is highly acknowledged for providing fellowship to one of the authors (Sandeep Nah Tripathi) and Indian Institute of Technology Delhi for all the facilities.

 

[1] S. Iijima, *Nature* **1991**, *354*, 56.
[2] M. Balkanski, *Mater. Sci. Eng. B* **2000**, *76*, 241.
[3] M. S. Dresselhaus, G. Dresselhaus, R. Saito, *Carbon* **1995**, *33*, 883.
[4] P. G. Collins, P. Avouris, *Sci. Am.* **2000**, *283*, 62.
[5] Z. Yao, H. W. C. Postma, L. Balents, C. Dekker, *Nature* **1999**, *402*, 273.
[6] H. V. Rizo, G. M. de Oca, I. R. Pastor, M. Monti, A. Terenzi, I. M. Gullon, *Compos. Sci. Technol.* **2012**, *72*, 218.
[7] H. J. Choi, S. J. Park, S. J. Kim, M. S. Jhon, *Diamond Relat. Mater.* **2005**, *14*, 766.
[8] S. N. Tripathi, P. Saini, D. Gupta, V. Choudhary, *J. Mater. Sci.* **2013**, *48*, 6223.
[9] C. McClory, T. McNally, M. Baxendale, P. Pötschke, W. Blau, M. Ruether, *Euro. Polym. J.* **2010**, *46*, 854.
[10] (a) A. Gupta, V. Choudhary, *J. Appl. Polym. Sci.*, **2012**, *123*, 1548; (b) A. Gupta, V. Choudhary, *Macromol. Symp.*, **2010**, *290*, 56.
[11] S.J. Park, M.S. Cho, S.T. Lim, H.J. Choi, *Macromol. Rapid Commun.* **2003**, *24*, 1070.
[12] S. T. Kim, J. Y. Lim, B. J. Park, H. J. Choi, *Macromol. Chem. Phys.* **2007**, *208*, 514.
[13] C. Velasco-Santos, A. L. Martinez-Hernandez, F. Fisher, R. Ruoff, V. M. Castano, *J. Phys. D: Appl. Phys.* **2003**, *36*, 1423.
[14] I. D. Rosca, F. Watari, M. Uo, T. Akasaka, *Carbon* **2005**, *43*, 3124.
[15] J. G. Wiltshire, A. N. Khlobystov, L. J. Li, S. G. Lyapin, G. A. D. Briggs, R. J. Nicholas, *Chem. Phys. Lett.* **2004**, *386*, 239.
[16] K. Behler, S. Osswald, H. Ye, S. Dimovski, Y. Gogotsi, *J. Nanopart. Res.* **2006**, *8*, 615.
[17] S. Osswald, M. Havel, Y. Gogotsi, *J. Raman Spectrosc.* **2007**, *38*, 728.
[18] F. Aviles, J. V. C. Rodriguez, L. M. Tah, A. M. Pat, R. V. Coronado, *Carbon*, **2009**, *47*, 2970.
[19] Z. Jin, K. P. Pramoda, G. Xu, S. H. Goh, *Chem. Phys. Lett.* **2001**, *337*, 43.
[20] N. K. Srivastava, B. B. Khatua, *Carbon*, **2011**, *49*, 4571.
[21] E. T. Thostenson, T. W. Chou, *J Phys D: Appl Phys*, **2002**, *35*, S77.
[22] P. Pötschke, A. R. Bhattacharyya, A. E. Janke, *Polym. J.* **2001**, *39*, 137.
[23] M. A. L. Manchado, L. Valentini, J. Biagiotti, *Carbon*, **2005**, *43*, 1499.
[24] S. D. Wanjale, J. P. Jog, *Polymer*, **2006**, *47*, 6414.
[25] Y. Li Huanga, Siu-ming. Yuen, *Compo. Sci. Tech.*, **2009**, *69*, 1991.
[26] K. W. Putz, C. A. Mitchell, R. Krishnamoorti, *J. Polym. Sci.*, **2004**, *39*, 2286.
[27] N. A. Kumar, J. Su Kim, Y. Seok, *Eur Polym J*, **2008**, *44*, 579.
[28] M. J. Li, X. B. Wang, R. Tian, F. M. Liu, H. T. Hu, R. Chen, H. Zheng, L. Wan, *Compos Part A Appl Sci Manuf*, **2009**, *40*, 413.
[29] S. J. Park, M. S. Cho, S. T. Lim, H. J. Choi, *Macromol Rapid Commun*, **2005**, *26*, 1563.
[30] M. G. Bindu, B. K. Satapathy, H. S. Jaggi, A. R. Ray, *Composites: Part B*, **2013**, *53*, 92.

 